PERGAMON

Journal of Structural Geology 23 (2001) 81–92

JOURNAL OF STRUCTURAL GEOLOGY

www.elsevier.nl/locate/jstrugeo

Quartz crystallographic and morphologic fabrics during folding/transposition in mylonites

F.D. Hongn[a], J.F. Hippertt[b]

[a]*CONICET, Facultad de Ciencias Naturales, Universidad Nacional de Salta, Buenos Aires 177, 4400 Salta, Argentina*
[b]*Departamento de Geologia, Universidade Federal de Ouro Preto, 35400-000, Ouro Preto, MG, Brazil*

Received 8 December 1998; accepted 26 April 2000

Abstract

Quartz grain shape fabrics (GSF) and *c*-axis lattice preferred orientation (LPO) were investigated in folded quartz ribbons with variable fold geometry in low metamorphic-grade granitic mylonites from northwestern Argentina. The folds, which vary from open to isoclinal, show an asymmetric short limb–long limb geometry developed simultaneously with the quartz fabrics during progressive simple shear. GSF shows a consistent obliquity relative to the bulk shear plane throughout the folded ribbons. GSF inclination varies between 25° and 45° oblique to the shear plane, indicating that relatively small finite strain increments ($\gamma \sim 1.2$) are attained before the GSF regeneration. In contrast, the *c*-axis preferred orientation varies throughout the folded ribbons. Unfolded ribbons and long limbs of folds show a typical *c*-axis maximum near the shear plane pole, while short limbs of tight and isoclinal folds show a *c*-axis maximum nearly orthogonal to that of long limbs. This pattern of domainal LPO is maintained in thickened ribbons derived from folding and transposition. This indicates that the GSF regeneration is comparatively much faster than a cycle of folding/transposition. Conversely, the LPO regeneration is much slower. We conclude that folding/transposition is a mechanism for development of domainal quartz LPO in kinematic frameworks with dominant simple shear.

1. Introduction

Natural and experimental deformation of quartz in shear zones has been extensively investigated in the last two decades (e.g. Brunel, 1980; Means, 1981; García Celma, 1982; Law et al., 1984; Hobbs, 1985; Burg, 1986; Mainprice et al., 1986; Dell'Angelo and Tullis, 1989; Cuevas and Tubía, 1990; Stünitz, 1991; Gleason and Tullis, 1995; Hippertt and Egydio-Silva, 1996 among many others). As a result of these studies, several processes of quartz intracrystalline deformation and their corresponding diagnostic features are known, including the origin and evolution of crystallographic and morphologic fabrics during dynamic recrystallization. However, the controls that enable crystallographic and morphologic fabrics to develop simultaneously during plastic deformation of quartz are still poorly understood.

Dynamically recrystallized quartz ribbons in low- to intermediate-temperature mylonites generally show an internal fabric defined by small, elongate grains disposed at angles of 20–45° to the mylonitic foliation, which has been referred to as *grain shape fabric* (GSF) (Brunel, 1980; Burg, 1986) or *Sb* (Law et al., 1984). It is presently recognized that processes such as dynamic recrystallization and preferred grain growth play an important role on the development of GSFs (see synthesis in Passchier and Trouw, 1996). Observation of naturally and experimentally produced GSFs (e.g. Lister and Snoke, 1984; Dell'Angelo and Tullis, 1989) indicates that these fabrics are successively reset during progressive deformation and, therefore, are interpreted to reflect the *XY*-plane of the instantaneous strain ellipsoid. The asymmetry of GSFs with respect to the bulk shear plane is also considered a reliable shear sense indicator (Simpson and Schmid, 1983)

Quartz ribbons in mylonites commonly display a well-developed lattice preferred orientation (LPO). At low metamorphic grade conditions (300–400°C), intracrystalline slip of quartz occurs preferentially through operation of basal $<a>$ glide (Bouchez, 1977). In cases where the finite deformation is high ($\gamma > 10$), the mylonitic foliation lies at a low angle to the bulk shear plane, which acts as a fabric attractor (Passchier, 1997). Because plastic deformation of quartz by basal $<a>$ glide progressively makes the (0001) planes of quartz subparallel to the bulk shear plane, a *c*-axis preferred orientation nearly perpendicular to the mylonitic foliation is produced. At these conditions, it is generally possible to assume that quartz basal planes and mylonitic foliation are parallel.

0191-8141/01/$ - see front matter
PII: S0191-8141(00)00051-1

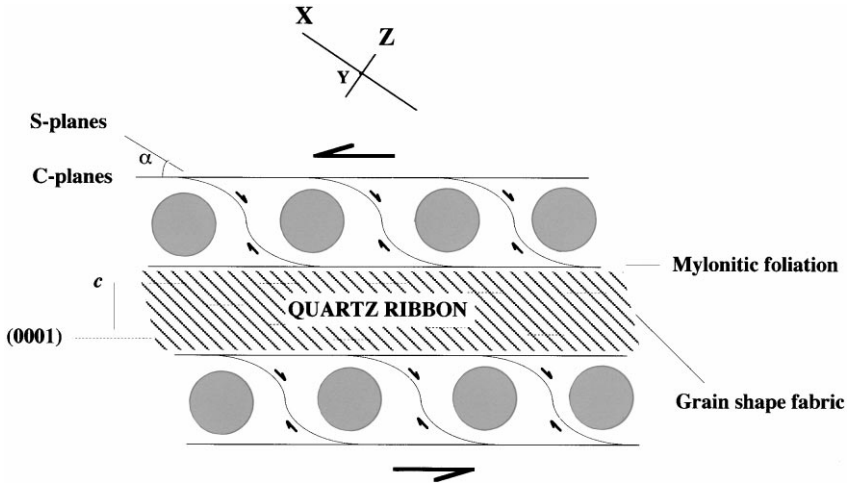

Fig. 1. Sketch illustrating deformational fabrics commonly present in banded mylonites, as observed in *XZ* sections. The circles represent rigid objects (porphyroclasts). The common orientation of *S*–*C* fabric, quartz *c*-axis fabric and GSF are indicated. *X*, *Y* and *Z* represent the instantaneous strain ellipsoid axes. The mylonitic foliation parallel to *C* planes is related to high finite shear strains ($\gamma > 10$).

Hanmer and Passchier (1991) suggested two main groups of fabrics in mylonites: strain-sensitive and strain-insensitive fabrics. Mylonitic foliations and crystallographic fabrics belong to the first group and GSFs to the second group. The most common geometric relationships between these usual rock fabrics in low metamorphic grade mylonites are summarized in Fig. 1. The origin and relationships between mylonitic foliation, quartz crystallographic fabric and GSF during progressive mylonitization have been interpreted in different ways. Brunel (1980) has explained the development of GSF as a consequence of a late deformation increment. In this view, the GSF is developed after the mylonitic foliation attains an orientation subparallel to the shear plane. Alternatively, GSFs are most commonly interpreted as a dynamic feature (or steady-state foliation), which represents an equilibrium between fabric-forming and fabric-destroying processes (Means, 1981; Dell'Angelo and Tullis, 1989; Herwegh and Handy, 1998).

García Celma (1982) analyzed domainal crystallographic and GSFs of quartz, recognizing domains which show opposite asymmetry (and, therefore, indicating an opposite shear sense) relative to the bulk shear. These domains of opposite asymmetry, which tend to disappear with progressive deformation, were interpreted as reflecting a component of pure shear in the overall kinematic framework. Such an interpretation is also adopted by Fueten et al. (1991). Variations of quartz crystallographic and shape fabrics related to folding have also been investigated (e.g. Carreras et al., 1977; Stünitz, 1991). These variations have been interpreted as indicating the operation of processes of passive folding and rotation of quartz fabrics (Carreras et al., 1977), as well as components of coaxial and simple shear deformation in different parts of folds (Stünitz, 1991).

In this paper, we investigate mylonites from the NW Argentina basement, which contain well-defined mylonitic zones developed at low metamorphic grade conditions (300–400°C). These mylonites generally contain well-developed microfolds, which are good examples for the investigation of relationships between crystallographic and GSFs during progressive ductile deformation and microfolding of quartz. The information presented herein is, in part, complementary to these previously mentioned studies. However, a new interpretation that relates quartz fabric variations with folding and transposition is proposed.

2. Geological setting

The investigated mylonites were formed in low metamorphic grade shear zones located in the Calchaquí Valleys basement, Province of Salta, NW Argentina. The Calchaquí Valleys basement consists of Neoproterozoic–Lower Cambrian low/medium grade metamorphites intruded by Lower Paleozoic plutonic rocks. The Calchaquí Valleys basement structure is complex as result of superposition of several deformation episodes since the Neoproterozoic–Lower Paleozoic (Mon and Hongn, 1996). The tectonic evolution of this basement shows two well-defined stages: (1) a first stage of Neoproterozoic–Paleozoic age, which includes at least two events of ductile deformation that originated its complex internal structure and; (2) a second stage of Cretaceous–Cenozoic age, which records events of brittle deformation related to the Cretaceous rifting and the Neogene Andean shortening (Mon and Hongn, 1996; Hongn and Seggiaro, 1998). Among the main structures of this basement, a regional system of ductile shear zones was developed during the Neoproterozoic–Paleozoic deformations (LeCorre and Rossello, 1994; Mon and Hongn, 1996). Most of these shear zones are conjugate, and may result from a transpressive tectonic regime in this region during the Lower Paleozoic (Hongn et al., 1996).

The Brealito shear zone (Fig. 2) is part of this regional

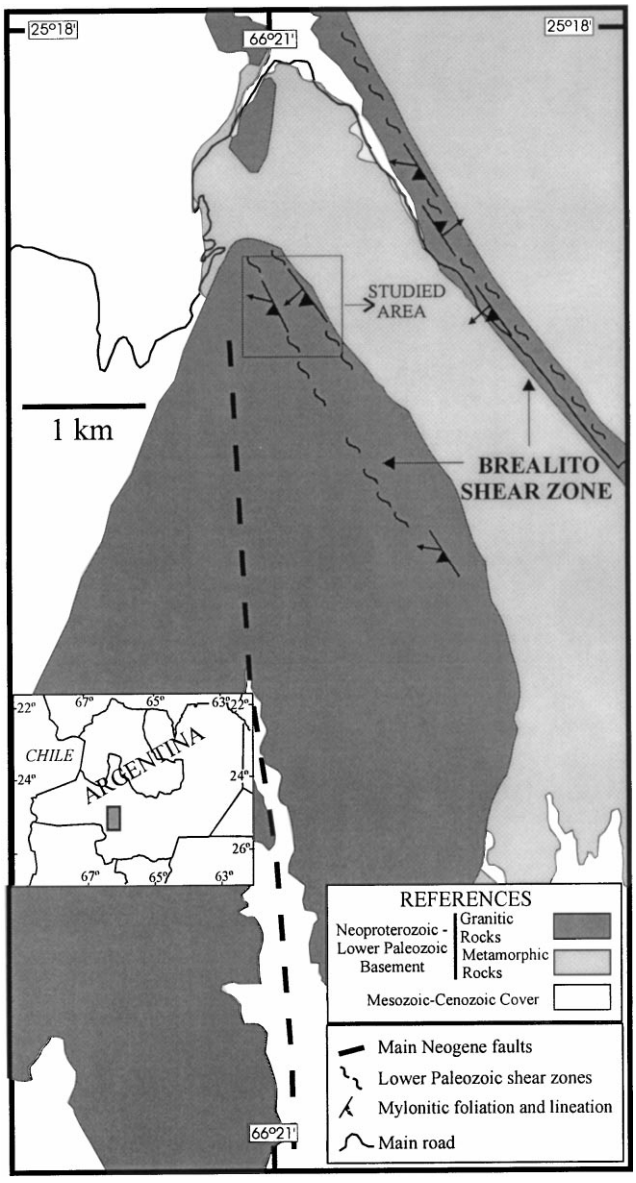

Fig. 2. Simplified geologic map showing the location of the Brealito shear zone in northwestern Argentina.

shear zone system. The Brealito basement consists of Neoproterozoic phyllites and schists intruded by an Ordovician (472 Ma; Lork and Balhburg, 1993) monzogranite. The Brealito shear zone consists of a set of minor shear zones distributed in a NW–SE-trending zone, which is 12 km long and 2 km wide. Cretaceous and Quaternary sediments cover the Brealito basement. The shear zones affect both granites and metamorphites but the deformational fabrics are clearly better-developed in the granite due to the lack of previous well-defined deformational structures in these rocks. The sampled mylonites came from shear zones in the eastern border of the granitic terrain (Fig. 2). The individual shear zones strike NW and dip approximately 70° SW. Their thicknesses vary from a few millimeters to more than a hundred meters.

3. Description of the rocks

The larger plutonic terrain (Fig. 2) is composed of a pink–gray porphyritic coarse-grained monzogranite. It contains K-feldspar megacrysts, up to 10-cm-long, immersed in a coarse-grained matrix composed of quartz, K-feldspar, plagioclase and micas, being biotite more abundant than muscovite. The composition of the mylonitic rocks is generally different from the protolith due to the intense fluid activity that produced modifications in both the chemical and mineralogical composition. Fluid activity on the lithological contacts was the main factor for strain softening and consequent localization of these shear zones. Fluid activity is also reflected by enrichment in quartz and tourmaline in relation to the protolith.

Mylonites show a well-defined planar fabric determined by alternating quartz-rich and mica-rich domains. The mica-rich domains contain most of the feldspar present in the rock. Locally, mylonites are transformed into 1-mm to 5-cm thick ultramylonite bands by a process of strain localization with cataclasis and reaction softening of feldspar as well as mass transfer of silica out of the ultramylonite bands (Hippertt and Hongn, 1998). The intense fluid activity enabled reaction softening that produced mica-enrichment in parallel with a decreasing content of feldspar. Most feldspar grains are inside the mica bands and show very fine-grained mica aggregates on their borders. Larger feldspar and tourmaline crystals are broken and displaced along the mylonitic foliation. The large, original mica crystals are almost totally transformed into very fine-grained mica, but some relics persist as mica-fishes. Quartz is totally concentrated in ribbons and will be described separately in the next section.

The mylonite fabrics show a strong asymmetry indicating that deformation had an important non-coaxial component at the scale of one millimetric, individual shear zone. Several kinematic indicators such as $S–C–C'$ fabrics, porphyroclast systems, mica-fishes and both crystallographic and GSFs of quartz record this general asymmetry. All indicators are consistent with each other and generally reflect reverse movements (thrusting) along a down-dip or oblique direction. However, on a thin section scale, opposite asymmetries defined by quartz *c*-axis fabrics are common. The description and interpretation of these asymmetries is one of the main goals of this paper.

Deformation occurred at low metamorphic grade conditions as indicated by the brittle behavior of feldspar and tourmaline, synkinematic growth of chlorite as a stable mineral and activation of basal $<a>$ glide in quartz. In addition, there is no evidence for subsequent static recrystallization of quartz. All these features are consistent with deformation at greenschist facies metamorphic conditions.

4. Quartz microstructures

In the investigated mylonites, quartz is almost totally

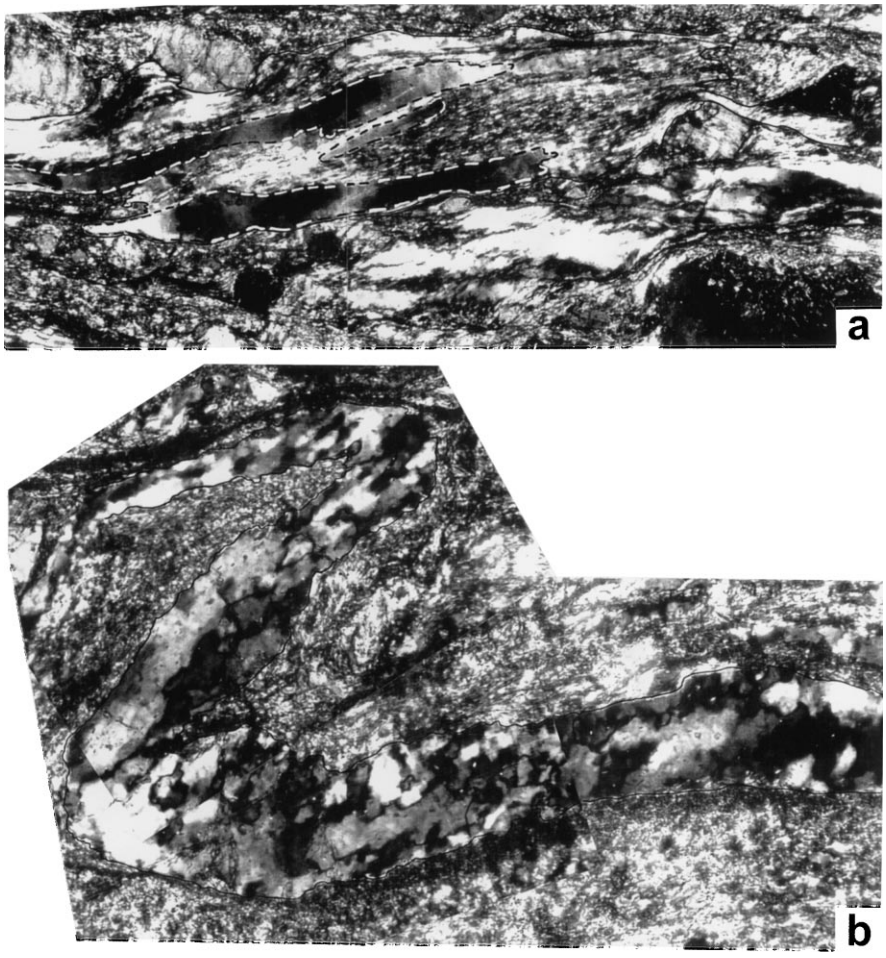

Fig. 3. Examples of dynamically recrystallized quartz ribbons showing different grain morphologies. (a) Ribbon comprised of elongate recrystallized grain aggregates and large monocrystalline domains, which are interpreted as a result of grain coalescence. Monocrystalline domains are outlined by black-and-white dashed line. Width of view is 3.2 mm (crossed nicols). (b) Ribbon comprised of equidimensional recrystallized grains with sutured boundaries, interpreted as formed by grain boundary migration recrystallization (GBMR). Width of view is 1.0 mm (crossed nicols).

segregated into ribbons, which show a variable geometry due to intense microfolding. In samples where the segregation is not complete, deformation produced a strong modification of the original quartz grains with development of undulose extinction, deformation lamellae, subgrains and new grains. In more deformed samples, all quartz is concentrated in entirely recrystallized ribbons and the original grains cannot be recognized anymore. Well-developed GSFs and *c*-axis fabrics are always present and indicate that dynamic recrystallization occurred during progressive deformation and stretching of these ribbons.

In *XZ* sections, quartz ribbons (Figs. 3 and 4) are generally continuous and extend from one side to another of the thin sections. They show an aspect ratio >30 and the thickness variation along a given ribbon is generally lower than 10% where they are not affected by folding. However, the ribbon thickness changes drastically where folding takes place. Thus, the thickness of some ribbons decreases twice or three times in the limits of a thin section or even fades out in some cases.

Quartz exhibits two main grain populations with characteristic sizes and shapes. More than 50% of the ribbon volume is generally composed by a population of small grains whose average size is between 10 and 30 μm, sometimes achieving 80 μm. These small grains can be separated into two subpopulations according to their shapes. Each population present features which are characteristic of different processes of dynamic recrystallization. Elongate grains with subparallel borders and small misorientation with subgrains of comparable dimensions and shapes (Fig. 3a) were probably originated by subgrain rotation recrystallization (SRR; White, 1979), while grains with sutured and irregular borders (Fig. 3b) were most probably originated by grain boundary migration recrystallization (GBMR; Urai et al., 1986). The coexistence of these different recrystallization processes in quartz is in fact common at low metamorphic conditions (FitzGerald and Stünitz, 1993). The new grains formed by GBMR are a few larger (50–80 μm) than those formed by SRR. In addition, there is also a possibility that all grains were originally formed by SRR, with some being subsequently modified or grown by GBM.

Between two consecutive domains of recrystallized grain

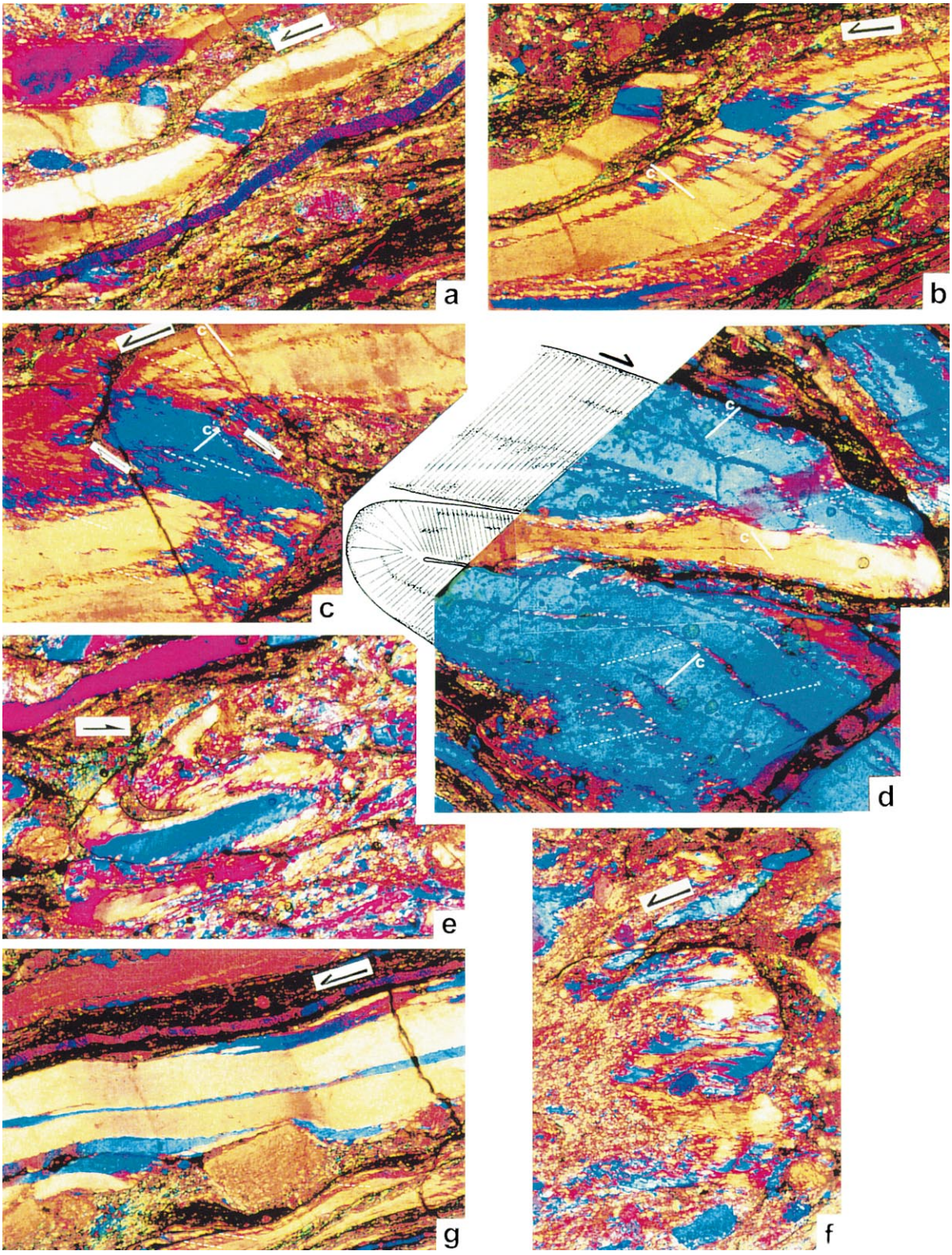

Fig. 4. Optical observation of folded quartz ribbons with variable fold geometries (gypsum plate inserted). The slow ray of the gypsum plate is oriented in the NE–SW direction. *c*-Axis traces (C), GSFs (dashed lines) and shear sense are indicated. (a)–(d) Progressive stages of fold closure. Note the perpendicular relationships of *c*-axes between short limbs and long limbs. The local, antithetic shear in the short limb is indicated in (c). (e)–(g) Transposed ribbons with domainal *c*-axis fabric. The microstructure in (e) shows a thick, transposed ribbon (with a domainal *c*-axis fabric) which is being re-folded. In (g), a pure quartz ribbon thickened by transposition is shown. The thin, blue domains with different *c*-axis orientation represent the short limbs of the precursor folds. Width of view is 2.5 mm in (a), (b), (c), (e) and (g); 2.8 mm in (d); 1.5 mm in (f).

aggregates, there are also large monocrystalline portions (e.g. Fig. 3a) whose dimensions do not correspond to that of the original quartz grains in the weakly deformed samples. Therefore, these large grains cannot be considered as porphyroclasts derived from original grains. Most of these large grains show a *c*-axis orientation similar to the adjacent recrystallized grains and do not show the typical sutured grain boundaries produced by GBM. These features suggest that this monocrystalline domains probably result from a process of grain-size enlargement due to coalescence of recrystallized grains aggregates with strong preferred orientation and, as a consequence, with small misorientation between adjacent grains (e.g. Herwegh et al., 1997). A selective grain growth by GBM it is not a likely explanation in this case, as the strong preferred orientation of the precursor aggregate, probably precludes large differences of stored plastic energy to exist between adjacent recrystallized grains to promote such an exaggerated grain growth by GBM (e.g. Takeshita et al., 1999).

Quartz shows a strong *c*-axis preferred orientation inside the ribbons. Most *c*-axes lie at low angles to the mylonitic foliation pole, indicating that plastic deformation of quartz occurred predominantly through activation of basal $<a>$ glide. Quartz GSF is also conspicuously developed. Most of the elongate new grains and subgrains, attributed to SRR, have their longest sides subparallel and disposed at angles of 25–45° to the unfolded ribbon boundary. Small grains with sutured boundaries, attributed to GBMR, are generally equidimensional and do not contribute to the GSF. However, since elongated recrystallized grains are much more abundant, the GSF is well-defined in most quartz ribbons.

Microfolding of the quartz ribbons is a key to determine how quartz crystallographic and GSFs change during progressive deformation. Although the investigated folds are on a microscale, they are sufficient large for determination of their hinge lines, which are at a high angle to the lineation observed in hand samples. So, it was possible to cut thin sections which are parallel to stretching lineation, normal to foliation and perpendicular or at high angles to the hinge lines for studying quartz fabrics variations related to folding.

Fold geometry varies from open folds or flexures (Fig. 4a, b) to tight and isoclinal folds (Fig. 4c, d). There appears to be no direct relationship between fold geometry and ribbon thickness since different fold geometries are common in both thin and thick ribbons. Much of these folds can be associated with a strong local rheological contrast where adjacent domains deform with different strain rates (Hippertt and Hongn, 1998). Folds are asymmetric with a short limb–long limb geometry (Fig. 4c, d). The fold asymmetry is always consistent with other shear sense indicators, indicating that quartz microfolding is associated to the same overall deformation that originated these mylonites. The long limbs generally correspond to domains that are less affected by folding. The thickness of the long limbs is regular but may vary near the hinge zones, where they are more affected by folding. The ribbon thickness varies in short limbs according to the limb orientation. Ribbons are thickened in short limbs of folds with interlimb angles greater than 90° (Fig. 4a), and are thinned in folds with interlimb angles lower than 90° (Fig. 4c). With interlimb angles close to 0°, which correspond to tight or isoclinal folds, the short limb thickness is smaller than in the long limb.

Folds with interlimb angles between 45° and 0° (i.e. tight and isoclinal folds) may show several degrees of transposition. Some tight or isoclinal folds have a thin, generally micaceous domain intercalated between the limbs. However, if this micaceous domain is absent, the final result of folding is a pure-quartz, thickened ribbon without impurities that mark the original limits of the ribbon. Some ribbons that fade suddenly out with rounded terminations, as well as ribbons that show abrupt thickness variations may also represent these transposed folds. If the ribbons have internal impurities such as a thin micaceous layer or a planar array of mica crystals, then the process of transposition can be most easily recognized. However, when they are composed of pure quartz, sometimes it is difficult to separate an originally thick ribbon from a thin ribbon thickened by folding. Fig. 4(d–g) shows microstructures recording these different stages of transposition.

5. Quartz fabric variations and microfolding

Folded quartz ribbons are a good natural laboratory to investigate fabric variations that occur in parallel with geometric modifications during progressive folding. In addition, these structures allow investigation of how fabric development and folding processes can interact and constrain each other. GSFs are most commonly considered as finite strain-insensitive structures, which reflect the orientation of the *XY*-plane of the instantaneous strain ellipsoid. In contrast, mylonitic foliation and crystallographic fabrics are considered as finite strain-sensitive structures that are progressively developed, and may reflect the orientation and shape of the finite strain ellipsoid (Hanmer and Passchier, 1991). However, when microfolding occurs, flow perturbations cause changes in the rock fabrics, hence inducing regeneration of orientations consistent with the superimposed instantaneous and finite strains. As the processes responsible for regeneration of the different rock fabrics take place at different ratios, variable geometric relationships between mylonitic foliation, GSFs and crystallographic fabrics are produced.

5.1. Mylonitic foliation

Fig. 5 shows the angular relationships between the GSF and the folded ribbon surface (mylonitic foliation) with respect to the bulk shear plane. The ribbon orientation shows a dispersion in relation to the shear plane. About 20% of the measured mylonitic foliation is subparallel to

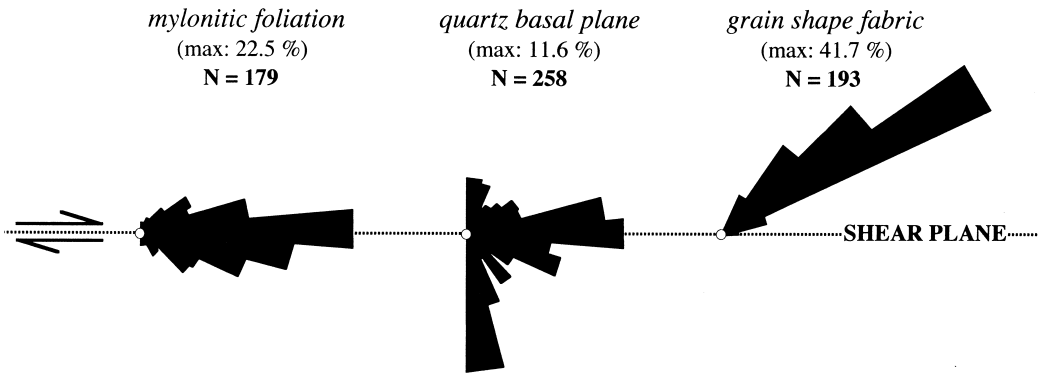

Fig. 5. Rose diagrams showing the orientation of mylonitic foliation, quartz basal planes and GSF relative to the bulk shear plane.

the overall shear plane indicating that, even when undergoing folding, the mylonitic foliation tends to maintain a low angle to the main shear plane. The other data are principally distributed between $+45°$ and $-45°$, recording the folded mylonitic foliation. These results show that the most stable mylonitic foliation orientation is at a low angle to the bulk shear plane. The scarcity of domains with obliquity greater than 45° is a consequence of the higher shear stresses resolved on the foliation plane at these orientations, which causes a comparatively quick reorientation of the mylonitic foliation towards more stable positions at smaller angles to the bulk shear plane.

5.2. Grain shape fabric

Grain shape fabric is not domainal as it always shows the same obliquity throughout any folded ribbon, except in zones of local flow anomalies such as adjacent to relatively rigid objects like feldspar porphyroclasts. The GSF exhibits a maximum concentration between 25° and 45° synthetically oblique to the bulk shear plane; i.e. the obliquity of this planar fabric is consistent with the overall non-coaxial kinematic framework as indicated by 80% of data (Fig. 5). Additional 20% laying out of the 25–45° range is related to flow anomalies in the vicinity of feldspar porphyroclasts. As folded ribbons show a consistent GSF over all the folded domains (including the hinge zones and inverted limbs), we infer that this fabric is continuously reset with a faster rate than the mylonitic foliation is reoriented. Although GSF is considered to reflect more efficiently the instantaneous strain ellipsoid than the finite strain ellipsoid, it appears that some finite strain increments are tracked by GSF before its regeneration. The GSF variation suggests that the GSF rotates from its initial position at 45° to the shear plane until a critical angle around 25° in the investigated mylonites (reflecting a finite strain increment $\gamma \sim 1.2$) where it is continuously reset to 45° by grain boundary migration (see also Ree, 1991), starting a new cycle.

5.3. Crystallographic fabric

Quartz developed a well-defined *c*-axis fabric during progressive deformation. In unfolded ribbons, quartz *c*-axes lie at high angles to the foliation plane indicating that most of quartz deformation occurred through basal $<a>$ glide. Rhomb and prism glides were less important, judging for the scarcity of *c*-axes in other orientations. Hence, an internal deformation of quartz principally achieved by basal $<a>$ glide is assumed. Fig. 6 shows that quartz basal planes and mylonitic foliation are nearly parallel in unfolded ribbons as well as in the long limbs of open folds. This relation is maintained in the hinge zones of open folds as well. The parallelism between basal planes of quartz and mylonitic foliation is observed in all folds with a short limb that is not inverted. After the short limb becomes orthogonal and its inversion starts, this parallelism is obliterated. If the basal planes of quartz undergo a passive rotation during folding of the quartz ribbons, we would expect to find a similar orientation of basal planes (and *c*-axes) in both limbs of isoclinal folds. However, quartz *c*-axis orientation in short limbs of tight and isoclinal folds is highly oblique, nearly normal in some cases, to that present in the long limbs. Then a change in the local deformation conditions must have occurred in the inverted limbs that inhibited the continued rotation of basal planes (discussed below).

Some 1–5-mm-thick ribbons show strong domainal crystallographic fabrics defined by alternating domains with different *c*-axis orientation. Some domains show the same orientation as unfolded ribbons or long limb of folds (*a*-domains of García Celma, 1982). Others show a *c*-axis orientation similar to that of short limbs of tight and isoclinal folds (*b*-domains of García Celma, 1982). The *a*-domains are generally thicker than the *b*-domains. Ribbons with well-defined domains of different crystallographic orientation, which are parallel to the ribbon surface (Fig. 4e–g) are generally thicker than ribbons without domainal fabrics, and may correspond to original thin ribbons thickened by a process of isoclinal folding and

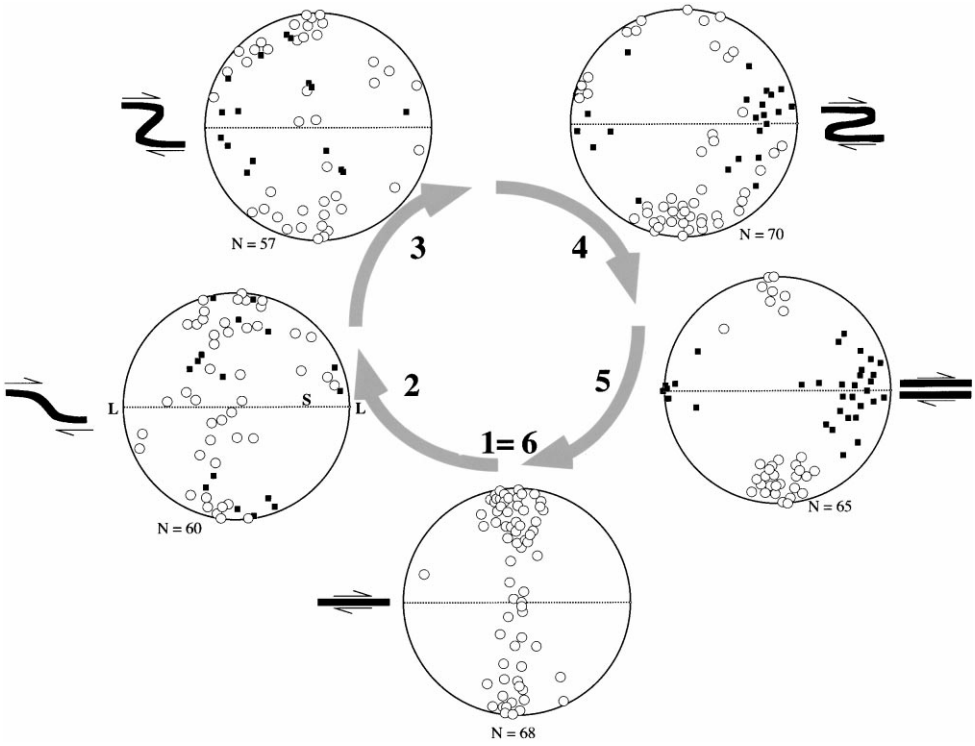

Fig. 6. Cyclic evolution of *c*-axis fabric during progressive folding/transposition. Note progressive development of a contrasting preferred orientation in the short limbs (black squares). Shear plane is vertical (E–W) and shear direction is horizontal in all diagrams. Circles represent *c*-axes measured in unfolded ribbons and long limbs of folds. $N = 320$.

transposition of quartz bands. Some quartz ribbons show a thinner portion without domainal LPO and a thicker one with domainal LPO.

6. Discussion

Our results indicate that all the studied fabrics (i.e. mylonitic foliation, GSF and *c*-axis fabric) are reset during progressive deformation, but at different rates. Thus, regeneration of GSF is the fastest one as indicated by the consistent asymmetry in all domains of a folded ribbon (Fig. 7). In contrast, regeneration of *c*-axis fabric (LPO) is the slowest, as indicated by the existence of domainal crystallographic fabrics even in ribbons where transposition of the quartz ribbons (mylonitic foliation) has already been completed. As a consequence, rate of mylonitic foliation regeneration is inferred to be intermediate between those of crystallographic and GSFs.

The schematic evolution of these structures is presented in Fig. 8, which synthesizes all observations about fabric variations during microfolding and transposition. The initial angle between mylonitic foliation and the overall shear plane is about 45° (Berthé et al., 1979; Passchier and Trouw, 1996), and decreases with progressive deformation. Mylonitic foliation and shear plane are subparallel above finite shear strains (γ) close to 10 (Herwegh et al., 1997). In steady-state flow, this angular relationship may be maintained along the whole deformation. However, flow perturbations (e.g. because of contrasting deformation rates in adjacent domains with different rheologic behaviors; Hippertt and Hongn, 1998) may cause folding. Folding generates a destabilization of the rock fabrics. As a consequence, the system immediately starts to recover the equilibrium by operation of mechanisms such as intracrystalline slip and grain boundary migration that reset the rock fabrics.

Quartz GSF develops in dynamically recrystallized aggregates and starts to form at relatively low finite shear strains (e.g. Dell'Angelo and Tullis, 1989), so when ribboning begins in a mylonite, GSF is already present. Because of its relatively constant orientation, GSF is considered as a finite strain-insensitive structure (Hanmer and Passchier, 1991). However, in the investigated mylonites, GSF records increments of progressive deformation as it is formed with an initial angle of 45° to the main shear plane, and rotate until an angle of 25–30° where it is reset, beginning a new cycle. Therefore, if GSF is passively rotated during progressive folding (e.g. Carreras et al., 1977), then it is 'sensitive' for finite shear strain increments (γ) about 1.2–1.3.

The results indicate that GSF regeneration is faster that the reorientation of the mylonitic foliation, as GSF does not show any significant variation through a folded ribbon with any geometry. The only changes observed are in the vicinity of large feldspar porphyroclasts where local flow perturbations generally occur (Fig. 7). When the mylonitic foliation

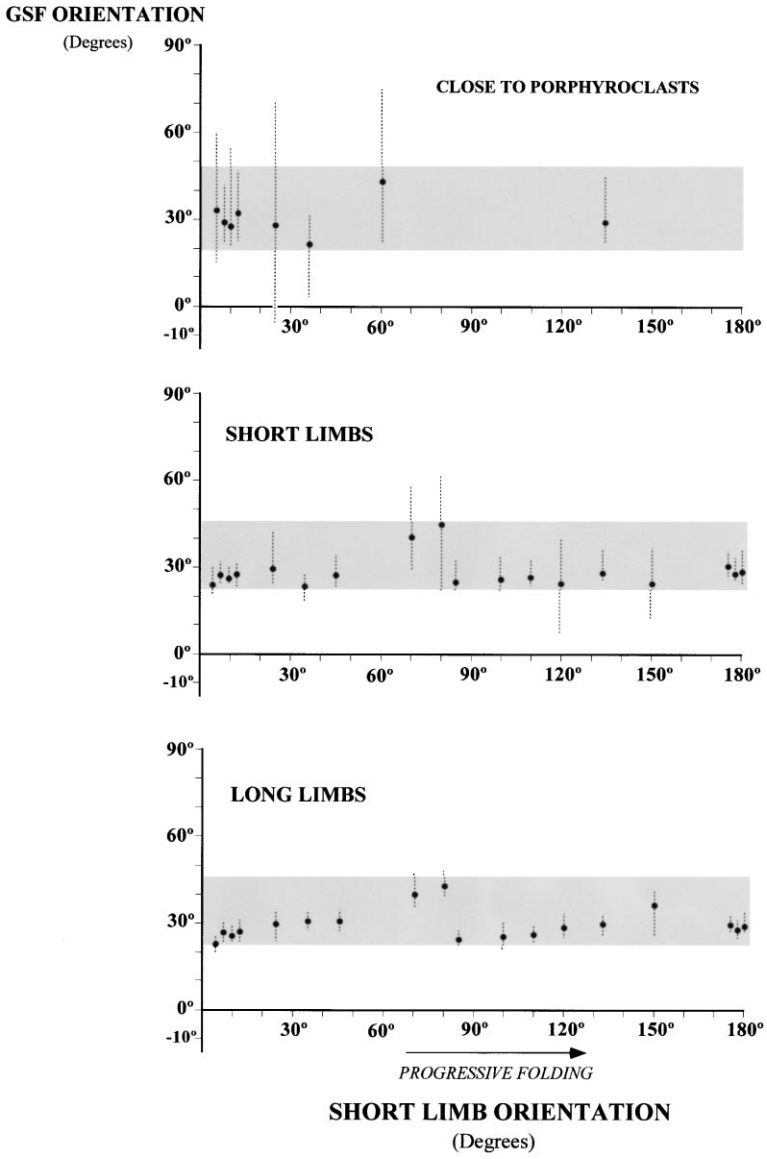

Fig. 7. Diagrams showing the variation of grain shape fabric (GSF) orientation relative to the bulk shear plane in folded quartz ribbons with different degrees of fold closure. The progressive fold closure is plotted as the orientation of the short limbs relative to the bulk shear plane (horizontal axis). 0° represents an unfolded ribbon, 90° is the point where the short limb is perpendicular to the bulk shear plane and 180° denotes a totally inverted short limb in an isoclinal fold. GSF variations were measured in long limbs, short limb and in domains adjacent to feldspar porphyroclasts. The average GSF orientation is the same in all domains, but note the largest variations close to porphyroclasts. Also, GSF variation is generally greater in short limbs than in long limbs of a given ribbon.

is disturbed by folding, a continuous process of regeneration begins which continuously tends to parallel the ribboned structure with the shear plane. During this process, folds become progressively tight, attain an isoclinal geometry and are subsequently transposed, regenerating the mylonitic foliation. The final result is formation of a thicker ribbon originated by the lateral joining of a short limb 'sandwiched' between two long limbs after fold transposition (e.g. Fig. 4e–g). This thickened ribbon is then stretched, folded again and transposed, cyclically. The complete process of folding/transposition is much slower than the GSF regeneration and several cycles of GSF regeneration may occur during the development of a single cycle of folding/transposition (Fig. 8).

The process of LPO regeneration begins with folding. Quartz LPO may appear at finite shear strains (γ) smaller than 2, and may be present even before the development of a well-defined ribboned structure (e.g. Dell'Angelo and Tullis, 1989). In the investigated mylonites, quartz ribbons already show a strong LPO at the deformation stage where folding begins. Initially, quartz basal planes are at a low angle to mylonitic foliation and they keep this parallelism even in hinge zones of open folds. However, they are not parallel in short limbs of more tight folds, and some change

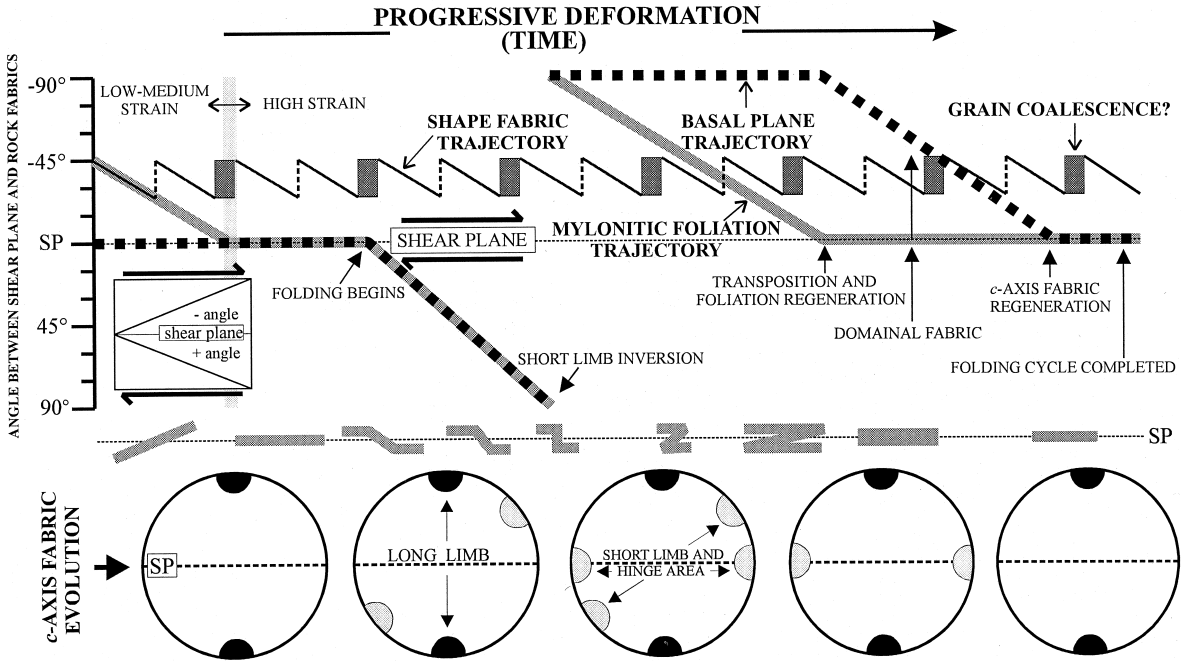

Fig. 8. Sketch summarizing the evolution of the different rock fabrics during progressive deformation. The kinks mark main changes in the fabric evolution (see text).

in the deformation conditions must have occurred in these domains to induce this modification. The key to answer this question may be in the local kinematics acting on the short limbs during progressive folding. As the short limbs of folds rotate towards the shear plane after their inversion, they are subjected to a local shearing which is opposite to the bulk shear (Fig. 9). Thus, there is a competition between the overall shear along the main shear plane and the local, opposite shear acting on the short limbs. As a result, rotation of quartz LPO is blocked and tend to be maintained in an equilibrium position where the basal planes lie in an orientation of equal extension in both the local and overall instantaneous strain ellipsoids. This is because, in this particular orientation, shear strains with comparable magnitudes (if we assume the overall and local strain ellipses having similar axial rates) but opposite senses tend to be accommodated in the basal planes. These two strain components annul each other preventing additional slip and rotation of the basal planes that, therefore, is stabilized in this orientation (Fig. 9). This position corresponds to the bisection of the greater angle between the bulk shear plane and the short limb plane. This position tends to be at a high angle to the bulk shear plane and does not vary significantly with progressive folding. In the short limbs, this blocking of the basal planes at a high angle to the overall shear plane should not favor continued stretching through basa l $< a >$ slip in these domains after transposition/thickening. Subsequent operation of prismatic glides, therefore, appears as a possible explanation. This is also corroborated by the presence of some secondary submaxima parallel to *Y*-axis of finite strain in Fig. 5. Alternatively, a thickened ribbon showing a domainal LPO produced by transposition (e.g. Fig. 4g) can evolve through progressive elimination of grains in 'hard-slip' orientations (previous short-limb domains) by grain boundary migration recrystallization (e.g. Herwegh and Handy, 1996). Because the regeneration of LPO is slower than the mylonitic foliation regeneration (through transposition), the transposed ribbons generally conserve a domainal LPO with alternating domains of different orientation which correspond to the short and long limbs of the precursor fold. This situation is maintained until the LPO regeneration is complete in domains derived from short limbs. However, it is possible in some cases that a new cycle of folding/transposition starts before the LPO reset is complete, as suggested by some microstructures (e.g. Fig. 4e). In summary, we suggest that the variable microstructures and textures present in a mylonite formed in progressive simple shear are largely controlled by the rate of regeneration of the different rock fabrics.

7. Conclusions

By examining the geometric relationships between grain shape fabric (GSF) and lattice preferred orientation (LPO) of quartz in folded quartz ribbons of a granitic mylonite, we have drawn three main conclusions:

1. GSF and LPO are reset at different rates during progressive plastic deformation and folding of quartz. GSF regeneration is much faster than progressive folding and subsequent transposition, and records short increments of

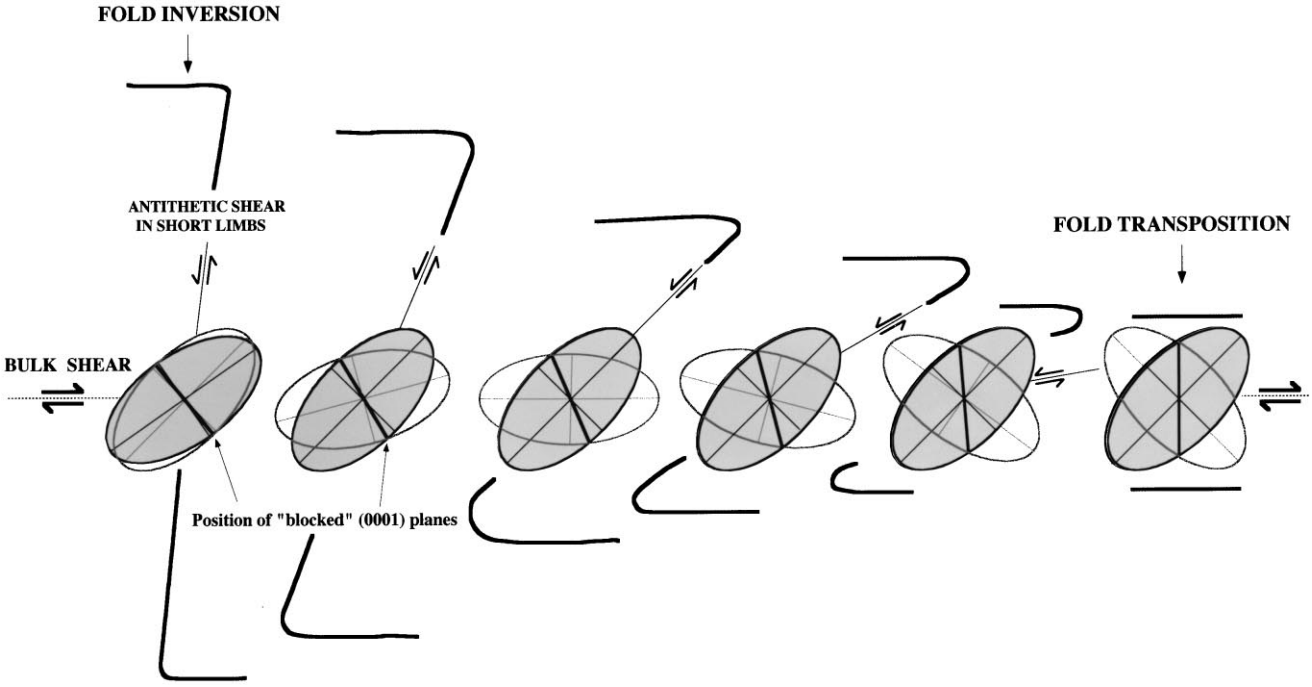

Fig. 9. Sketch showing the evolving orientation of the instantaneous strain ellipses related to the overall shear (dotted) and local antithetic shear (blank) in short limbs of folds during progressive folding/transposition. The black, thick lines mark the direction of intersection between the two ellipses in each stage, where basal planes of quartz tend to be 'blocked'. Note that, while the short limb rotates 90° from its inversion up to transposition, the basal planes of quartz rotate only 45°. As a result, domainal crystallographic fabrics may be preserved after fold transposition.

shear strain ($\gamma \sim 1.2$) which account for the orientation range between 45° and 25° oblique to the shear plane.

2. Because of local strain heterogeneities due to competing overall and local strains, the LPO tends to attain a stable orientation in inverted limbs of folds making LPO regeneration to occur at lower rates than progressive folding/transposition. This causes the transposed ribbons to preserve a domainal LPO which reflects the orientation of short and long limbs of the precursor fold.
3. The existence of domainal quartz LPO in tectonites, commonly interpreted as indicating a component of coaxial deformation, may in some cases result from folding/transposition in a kinematic framework with a dominant component of simple shear.

Acknowledgements

Financial support for this research was provided by CIUNSa and CONICET (PEI 0427/97; PIP 5020) grants to Hongn; and CNPq (process 523688/96-2) and FAPEMIG research grants to Hippertt. J. Tubía is thanked for suggestions and criticisms. Constructive journal reviews were made by J. Ree and an anonymous reviewer. This does not imply that they agree with all of our points of view.

References

Berthé, D., Choukroune, P., Jegouzo, P., 1979. Orthogneiss, mylonite and non-coaxial deformation of granites: the example of the South Armorican shear zone. Journal of Structural Geology 1, 31–42.

Bouchez, J.L., 1977. Plastic deformation of quartzites at low temperature in an area of natural strain gradient. Tectonophysics 39, 25–50.

Brunel, M., 1980. Quartz fabrics in shear zone mylonites: Evidence for a major imprint due to late strain increments. Tectonophysics 64, 33–44.

Burg, J.P., 1986. Quartz shape fabrics variations and *c*-axis fabrics in a ribbon-mylonite: arguments for an oscillating foliation. Journal of Structural Geology 8, 123–131.

Carreras, J., Estrada, A., White, S., 1977. The effects of folding on the *c*-axis fabric of a quartz mylonite. Tectonophysics 39, 3–24.

Cuevas, J., Tubía, J.M., 1990. Quartz fabric evolution within the Adra Nappe (Betic Cordilleras, Spain). Journal of Structural Geology 12, 823–833.

Dell'Angelo, L.N., Tullis, J., 1989. Fabric development in experimentally sheared quartzites. Tectonophysics 169, 1–21.

García Celma, A., 1982. Domainal and fabric heterogeneities in the Cap de Creus quartz mylonite. Journal of Structural Geology 4, 443–455.

Gleason, G.C., Tullis, J., 1995. A flow law for dislocation creep of quartz aggregates determined with the molten salt cell. Tectonophysics 247, 1–23.

FitzGerald, J., Stünitz, H., 1993. Deformation of granitoids at low metamorphic grade, I: Reactions and grain size reduction. Tectonophysics 221, 269–297.

Fueten, F., Robins, P.Y.F., Stephens, R., 1991. A model for the development of a domainal quartz *c*-axis fabric in a coarse-grained gneiss. Journal of Structural Geology 13, 1111–1124.

Hanmer, S., Passchier, C.W., 1991. Shear sense indicators: a review. Geological Survey of Canada. Paper 90, 1–71.

Herwegh, M., Handy, M., Heilbronner, R., 1997. Temperature- and

strain-rate-dependent microfabric evolution in monomineralic mylonite: evidence from in situ deformation of norcamphor. Tectonophysics 280, 83–106.

Herwegh, M., Handy, M.R., 1996. The evolution of high-temperature mylonitic microfabrics: evidence from simple shearing of a quartz analogue (norcamphor). Journal of Structural Geology 18, 689–710.

Herwegh, M., Handy, M.R., 1998. The origin of shape preferred orientations in mylonite: inferences from in-situ experiments on polycrystalline norcamphor. Journal of Structural Geology 20, 681–694.

Hippertt, J.F., Egydio-Silva, M., 1996. New polygonal grains formed by dissolution-redeposition in quartz mylonite. Journal of Structural Geology 18, 1345–1352.

Hippertt, J.F., Hongn, F.D., 1998. Deformation mechanisms in the mylonite/ultramylonite transition. Journal of Structural Geology 20, 1435–1448.

Hobbs, B.E., 1985. The geological significance of microfabric. In: Wenk, R.H. (Ed.), Preferred orientation in deformed metals and rocks. Academic Press, Orlando, pp. 463–484.

Hongn, F.D., Seggiaro, R.E., 1998. Mapa Geologico Hoja Cachi. Servicio Geológico Minero Argentino Map 2566-III, scale 1:250,000.

Hongn, F.D., Mon, R., Cuevas, J., Tubía, J.M., 1996. Zones de cisaillement calédoniennes à haute température dans la quebrada Barranquilla (Puna Orientale, Argentina): données structurales et cinématiques. Comptes Rendus Academie de Sciences de Paris, Série IIa 323, 809-815.

Law, R.D., Knipe, R.J., Dayan, H., 1984. Strain path partitioning within thrust sheets: Microstructural and petrofabric evidence from the Moine thrust zone at Loch Eriboll, northwest Scotland. Journal of Structural Geology 6, 477–497.

LeCorre, C., Rossello, E., 1994. Kinematics of Early Paleozoic ductile deformation in the basement of NW Argentina. Journal of South American Earth Sciences 7, 301–308.

Lister, G.S., Snoke, A.W., 1984. *S–C* mylonites. Journal of Structural Geology 6, 617–638.

Lork, A., Balhburg, H., 1993. New monazite U/Pb ages on granitoids of NW Argentina. Proceedings of 12th Argentinean Geological Congress 3, 12–19.

Mainprice, D., Bouchez, J.L., Blumefeld, Ph., Tubía, J.M., 1986. Dominant *c*-slip in naturally deformed quartz: Implications for dramatic plastic softening at high temperature. Geology 14, 819–822.

Means, W.D., 1981. The concept of steady-state foliation. Tectonophysics 78, 179–199.

Mon, R., Hongn, F.D., 1996. Estructura del basamento proterozoico y paleozoico inferior del norte argentino. Revista de la Asociación Geológica Argentina 51, 1–10.

Passchier, C.W., 1997. The fabric attractor. Journal of Structural Geology 19, 113–127.

Passchier, C.W., Trouw, R.A.J., 1996. Microtectonics. Springer-Verlag, Heidelberg.

Ree, J., 1991. An experimental steady-state foliation. Journal of Structural Geology 13, 1001–1011.

Simpson, C., Schmid, S.M., 1983. An evaluation of criteria to determine the sense of movement in sheared rocks. Geological Society of American Bulletin 94, 1281–1288.

Stünitz, H., 1991. Folding and shear deformation in quartzite, inferred from crystallographic preferred orientation and shape fabrics. Journal of Structural Geology 12, 71–86.

Takeshita, T., Wenk, H.R., Lebensohn, R., 1999. Development of preferred orientation and microstructure in sheared quartzite: comparison of natural data and simulated results. Tectonophysics 312, 133–155.

Urai, J.L, Means, W.D., Lister, G.S., 1986. Dynamic recrystallization of minerals. In: Hobbs, B.E., Herad, H.C. (Eds.), Mineral and Rock Deformation: Laboratory Studies—The Paterson Volume, Geophysical Monograph, 36. American Geophysical Union, pp. 61–199.

White, S.H., 1979. Grain and sub-grain size variations across a mylonite zone. Contributions to Mineralogy and Petrology 70, 193–202.